LTE-Advanced Downlink Throughput Evaluation in the 3G and TV White Space Bands

Araz S. Ameen, Evangelos Mellios, Angela Doufexi, Naim Dahnoun and Andrew R. Nix

Communication Systems & Networks Group, Department of Electrical and Electronic Engineering
University of Bristol, Bristol, United Kingdom

Email: {Araz.Ameen, Andy.nix}@bristol.ac.uk

***Abstract*—To maintain a high quality of service to the increasing number of smartphone users, additional spectrum is required. The TV white space bands provide a good opportunity to achieve this goal. They can be used as standalone spectrum or aggregated with other licensed bands to increase the total available bandwidth. This paper compares the downlink throughput performance of LTE-Advanced in two different frequency bands. It also addresses the impact of smartphone orientation, with results quoted for three different elevation angles. We consider the higher LTE-Advanced band at 2.6 GHz and the TV white space band at 800 MHz. The radio channel is modelled using a state-of-the-art 3D ray-tracing tool combined with measured 3D radiation patterns for the base station and handset antennas. The throughput performance for a large number of base station and mobile terminal locations is investigated in two different UK cities. We use the computationally efficient received bit information rate algorithm to compute packet error rate as a function of channel structure and SNR. The approach reduces simulation run time by a factor of more than 300. Similar average throughput vs SNR results are observed in both frequency bands. However, higher K-factor and total received power levels are observed when the user equipment is tilted to 45º in elevation. Throughput results show that the efficiency of carrier aggregation between LTE and TVWS bands depends on the cell size and the type of urban environment.**

***Index Terms*—LTE; TVWS; RBIR; Carrier Aggregation**

I. INTRODUCTION

The target of 2G and 3G mobile operators is to support voice and IP services to a wide range of mobile devices. Recent capacity demands have led to the evolution of LTE to LTE-Advanced (4G). Bandwidth flexibility (from 1.4 MHz to 20 MHz) is one of the main characteristics of LTE. This allows radio access deployment in different frequency bands, each of which has their own unique characteristics [1].

Carrier aggregation (CA) up to five times the standard LTE bandwidth is supported in LTE-Advanced to achieve a maximum downlink (DL) data rate of 1 Gbps and uplink (UL) data rate of 500 Mbps. CA_7-20 denotes inter-band carrier aggregation between EUTRA bands 7 and 20 for UL and DL as planned by the 3GPP technical specification group for Release 11 of the LTE standard [2]. The selection of 800 MHz and 2.6 GHz in this study is based on the DL frequency range of bands 20 and 7 respectively.

Recent research has explored how best to access additional spectrum. A number of studies have focused on the use of unlicensed 60 GHz bands. Although at these frequencies large amounts of new spectrum are available, propagation path loss is extreme [3]. Utilizing the unused licensed VHF and UHF bands of digital terrestrial television (DTT), known as TV White Space (TVWS), is another important method to increase spectrum. The RF propagation performance in the TVWS bands is much better than the higher frequency cellular bands commonly in use today [4]. According to [5], after completing the digital switchover, 256 MHz of interleaved UHF spectrum will be available in the United Kingdom for digital terrestrial television (DTT). The utilization of these TV channels depends on the geographic region and time.

Currently geo-location databases are proposed to decide whether a certain channel is occupied or available for TVWS transmission [6]. No previous publications have compared the performance of LTE-Advanced in the 2.6 GHz cellular and the 800 MHz TVWS band. Furthermore, no studies have considered carrier aggregation using TVWS spectrum. In this paper a received bit information rate (RBIR) abstraction technique is used to quantify the DL throughput for an LTE-Advanced single antenna system. Results are generated for large numbers of urban users in an interference-free scenario. Measured 3D antenna patterns for the macro-cell base stations (BS) and the user equipment (UE) handsets are integrated with a 3D ray tracing tool [7] to model the antenna/channel combination at carrier frequencies of 800 MHz and 2.6 GHz. Two propagation environments and three handset elevation angles are considered.

The remainder of this paper is organized as follows: The channel model parameters are described in Section II. Section III first verifies the RBIR technique and then presents the LTE-Advanced link level simulation results. The throughput performance results are presented in Section VI, and conclusions are drawn in Section V.

II. CHANNEL MODEL PARAMETERS

The channels in this paper are created using a ray tracing tool based on an urban site specific database [7]. The ray tracing engine identifies all possible ray paths between the transmitter and the receiver in 3D space. The database includes terrain, buildings and foliage. This deterministic approach is preferred over the standardized SCM 3GPP LTE channel model [8] since the latter makes several simplifying assumptions which include simplified angle spread distributions, propagation restricted to the azimuth plane, and no mechanism for modelling specific 3D antenna patterns.

978-1-4577-1348-4/13/$31.00 ©2013 IEEE

Within the ray tracer, 23 macro-cell BSs were placed on rooftop locations in two different urban environments; a (4 km x 4.4 km) area in the city centre of Bristol, UK, and a (11 km x 13 km) area in the centre of London, UK. Each base station was modelled to cover a 3-sector cell with a radius of 1 km. 300 UEs were randomly scattered at street level within each sector. The system was modelled at carrier frequencies of 800 MHz and 2.6 GHz using measured BS and UE antenna pattern. The total power radiation patterns are shown in Fig. 1 [9]. The orientation of the UE will be shown to have a significant impact on the BS-UE propagation characteristics [10], therefore three different UE antenna orientations (elevation=0º, 45º, 90º) are considered. Table I summarises the channel model parameters.

The channel model propagation statistics are shown in Fig. 2, which includes the cumulative distribution function (CDF) of the total received signal power, the K-factor, the root mean square (RMS) delay spread, and the RMS angle of departure (AoD) and angle of arrival (AoA) in the azimuth and elevation spreads. This is a DL study and hence departure angles represent the BS, while arrival angles represent the UE. The results in Fig. 2 are divided by geographic region into Bristol (left hand side) and London (right hand side).

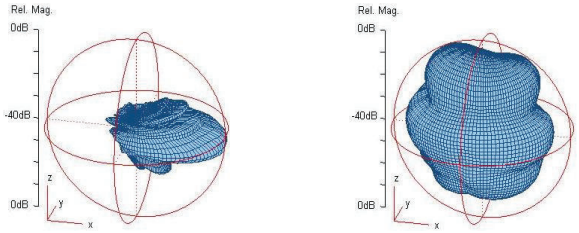

(a) Macro BS antenna (b) UE handset antenna

Fig.1. Total power measured radiation patterns.

TABLE I
CHANNEL MODEL PARAMETERS

Parameter		Value
LTE Advanced Bandwidth		10 MHZ
Carrier Frequency		800 MHz, 2.6 GHz
Number of BS		23
Number of Sectors		3
Number of UE per Sector		300
BS heights (m)	Bristol	24, 31, 33, 10, 27, 27, 34, 45,77, 50, 9, 7, 28, 13,7, 10, 21, 30, 23, 9, 48, 28, 12
	London	25, 61, 18, 18, 43, 26, 15, 24, 37, 59, 114, 74, 30, 92, 8, 57, 122, 60, 82, 58, 43, 28,49
UE height (m)		1.5
UE locations		50 m-1000m from BS
BS transmit power (dBm)		43
BS antenna type		6 dual polarised uniform linear array
UE antenna type		(Omni-directional) NOKIA mobile phone
Antenna 3dB azimuth/elevation beamwidth	BS	65º/15º
	UE	360º/36º
BS antenna downtilt		10º
UE rotation		Azimuth = 0º, Elevation = 0º, 45º, 90º
User mobility (m/s)		0

Comparing the results in Fig. 2 in terms of carrier frequency, it can be seen that considerably higher RF signal levels occur at 800MHz. Both frequencies have approximately the same K-factor, with slightly higher values observed at 2.6 GHz in Bristol. Lower RMS spreads are observed at 2.6 GHz in Bristol; however similar values are seen in the London scenario. Bristol differs from London in that it is very hilly. Furthermore, the average building height is higher in London. The net result is a lower total received signal power at the UEs in Bristol. In addition, it can be seen from Table I that the London BSs are higher than the Bristol BSs, which results in an increased probability of LOS.

UE antenna elevation is shown to have a significant effect on the total received power and the K-factor. Better performance is achieved for a UE elevation orientation of 45º. The RMS spreads (except AoA RMS azimuth spread) are not sensitive to UE elevation rotation. They only depend on the local scatters.

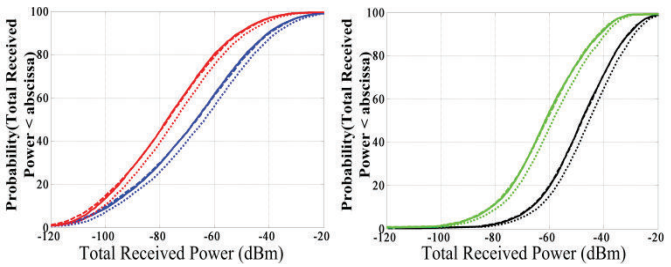

a) Total received power

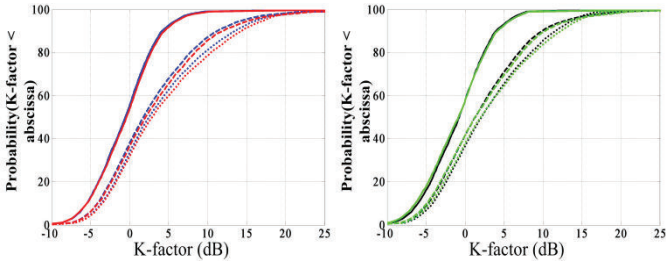

b) K- factor

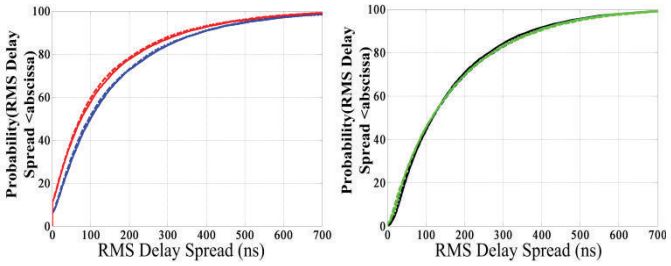

c) RMS delay spread.

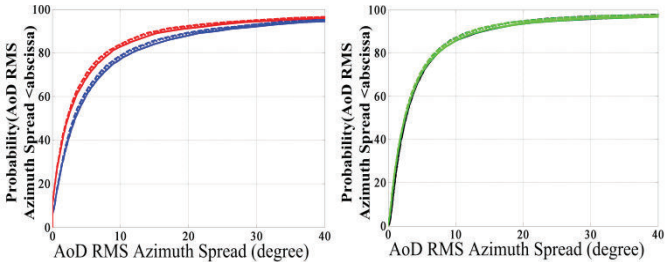

d) AoD RMS azimuth spread.

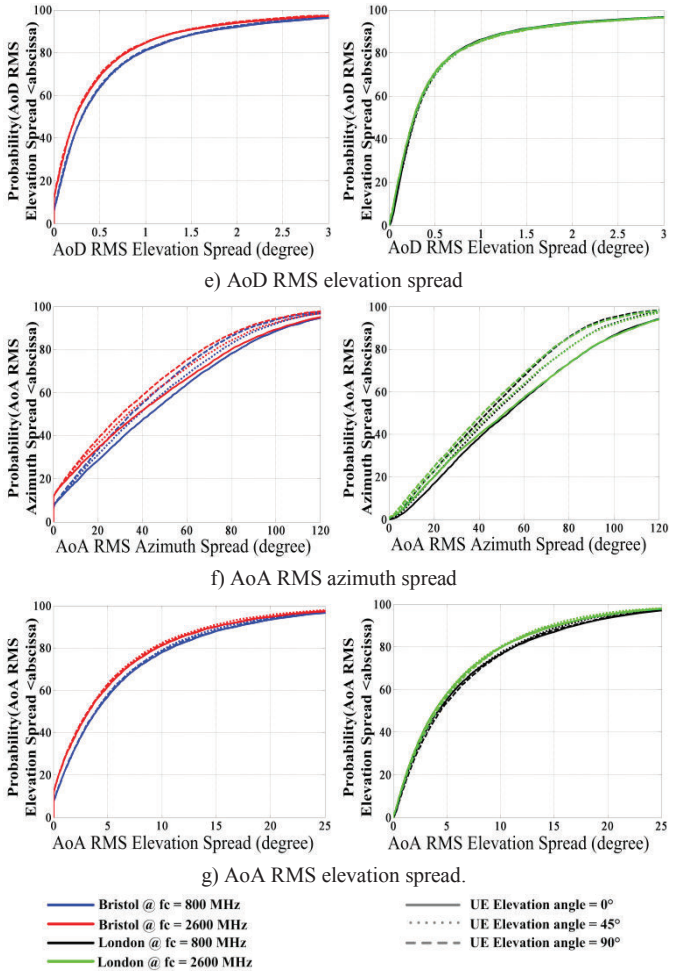

Fig. 2. Propagation statistics of the Ray Tracer channel model.

III. RBIR Link Level Simulation Results

Performing accurate physical layer bit accurate simulations for large numbers of BS and UE and for many different modulation and coding schemes (MCS) is time consuming. The RBIR technique [11] can be used as a computational efficient alternative to bit level simulation when studying the system level performance of a communication system. In OFDM systems, there are large SNR variations across the sub-carriers as results of frequency selective fading. Effective SNR Mapping (ESM) is used to convert the SNR vector into a single effective SNR (ESNR) using (1).

$$ESNR = \Phi_m^{-1}\left\{\frac{1}{N.N_{ss}}\sum_{n=1}^{N}\sum_{k=1}^{N_{ss}}\Phi\left(SNR_{n,k}\right)\right\} \quad (1)$$

The value $SNR_{n,k}$ represents the post-processing signal to noise ratio (SNR) for the k^{th} spatial stream of the n^{th} sub-carrier and m represents the modulation order. N represents the number of sub-carriers in the block, N_{ss} is the maximum number of spatial streams, and $\Phi(\bullet)$ is an invertible function. For mutual information (MI) ESM approach $\Phi(\bullet)$ is defined as the symbol information (SI) as given in (2).

$$SI(\gamma, m) = E_{XY}\left\{\log_2 \frac{P(Y|X,\gamma)}{\sum_X P(X)P(Y|X,\gamma)}\right\} \quad (2)$$

In (2) Y denotes the received symbol with input SNR equal to γ and $P(Y|X,\gamma)$ is the AWGN channel transition probability density conditioned on the noise-free transmit symbol X. $P(X)$ is assumed to be $1/m$. Then instantaneous bit error rate (BER) or packet error rate (PER) can be computed by mapping the ESNR using a look-up-table containing BER or PER performance versus SNR for an AWGN channel. This table can be obtained from bit accurate simulation.

Fig. 3 shows the block diagram of the transmitter in our LTE-Advanced downlink physical layer simulator. The reverse operations are performed at the receiver. To verify the accuracy of the RBIR abstraction engine, BER versus SNR performance was obtained for a single antenna system using our RBIR and bit accurate simulators. The simulation was performed for two UE locations; location1 with line-of-sight (LOS) (blue colour graphs) and location2 with non-LOS (brown graphs). The channel parameters at these two locations are listed in Table II.

Table III lists the modulation order, coding rates and data rates of the 10 MCS modes considered in this paper; however for clarity Fig. 4 shows the simulation results for just 3 MCS modes. A good match can be observed between the bit level and RBIR abstraction simulations. In order to compare the required run time for each simulator, PER simulations were performed in the SNR range -5 dB to 25 dB, with steps of 0.5 dB, for 10 MCS modes, 1000 independent channel snap-shots and for a 300 byte packet size. The run time for the bit level simulator was 57 hours, while the RBIR algorithm required just 11 minutes. The RBIR algorithm is more than 300 times faster. This speed-up is very important when studying thousands of UE and BS locations, along with different antenna orientations, operating environments, carrier frequencies and other channel parameters.

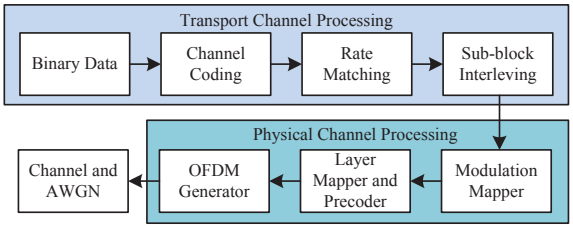

Fig. 3. Block diagram of the LTE-Advanced downlink transmitter.

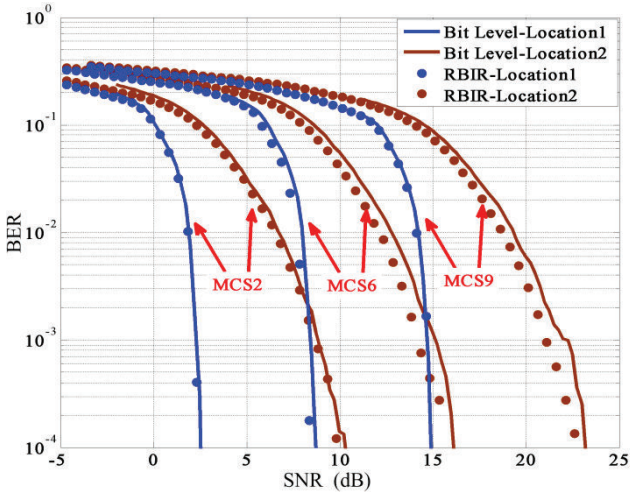

Fig. 4. BER comparison between Bit level and RBIR simulator.

TABLE II
CHANNEL MODEL PARAMETERS FOR THE TWO UE LOCATIONS IN FIG. 4

Parameter	Location1	Location2
Channel length	7	34
K-factor (dB)	17.2	-9
RMS Delay Spread(ns)	21.2	765.7
AoD RMS Azimuth Spread(degrees)	0.73	3.17
AoD RMS Elevation Spread(degrees)	0.001	0.53
AoD RMS Azimuth Spread(degrees)	8.14	70
AoD RMS Elevation Spread(degrees)	3.13	17.27

TABLE III
LIST OF MCS MODES

MCS	Modulation	Code rate	Data Rate (Mbps)
1	QPSK	1/3	5.6
2		1/2	8.4
3		2/3	11.2
4		4/5	14.44
5	16QAM	1/2	16.8
6		2/3	22.4
7		4/5	26.88
8	64QAM	2/3	33.6
9		3/4	37.8
10		4/5	40.32

IV. THROUGHPUT SIMULATION RESULTS

This section presents throughput results for LTE-Advanced single antenna systems using the RBIR simulator. Fig. 5 shows the throughput envelope of the 10 MCS modes as a function of SNR when averaged over *all* the UEs from *all* 23 macro-cells for 12 different cases. It is clear that both frequency bands have the same average throughput envelope; this similarity is related to the slight difference in the related channel statistics of Fig. 2(b - g). However, better performance is observed in the SNR range (5 dB – 25 dB) for UE antenna orientations of 45º and 90º due to the higher K-factor (see Fig. 2b).

Fig. 6 shows the CDF of the throughput for *all* UEs in the 23 macro-cells. The total number of UEs included in this study for the two cities and two frequency bands are listed in Table VI. The throughput at each UE was calculated by mapping the average SNR of that UE to its specific throughput envelope, which was obtained using the RBIR simulator. The UE average SNR was calculated using (3) [12]

$$SNR\ (dB) = P_{RX} - KTB\ (dBm) - NF\ (dB), \qquad (3)$$

where P_{RX} represents UE average received power, K is Boltzmann's constant, T is the temperature in Kelvin, B is the effective bandwidth (90% of the total bandwidth), and NF is the noise figure. For each LTE-Advanced UE, T=15°C (288 Kelvin) and NF=9 dB [13]. It can be observed from Fig. 6 that the throughput at 800 MHz is higher than that at 2.6 GHz due to the higher total received power in the lower frequency band (see Fig. 2a).

Comparing the CDF graphs of Fig. 6 in terms of UE antenna elevation, higher throughputs are observed for elevation angles of 45º (and to a lesser degree 90º) due to the improved K-factor statistics for these orientations (as shown in Fig. 2b). The sensitivity of the throughput to the UE orientation depends on operating frequency band and environment. For example, higher throughput enhancement can be observed from Fig. 6 for the 2.6 GHz band (relative to the 800 MHz band) and for Bristol relative to London.

The throughput coverage map of Bristol and London for one macro cell at two different frequencies and two different UE elevations (0º and 45º) are shown in Fig. 7. The effect of the different frequency bands and different antenna orientation on some UE locations can be seen clearly. Although not shown, the coverage maps at elevation angles of 0º and 90º are very similar (hence only the maps for 0º elevation is shown in Fig. 7. This can be seen from the close alignment of the CDF throughout graphs in Fig. 6.

It is clear from Fig. 7 that performing CA between the two frequency bands (left side of the figure with the right side) to increase channel capacity is more efficient in London than in Bristol for the macro cell. CA can offer increased capacity in Bristol for a smaller cell radius or for one sector of the macro-cell.

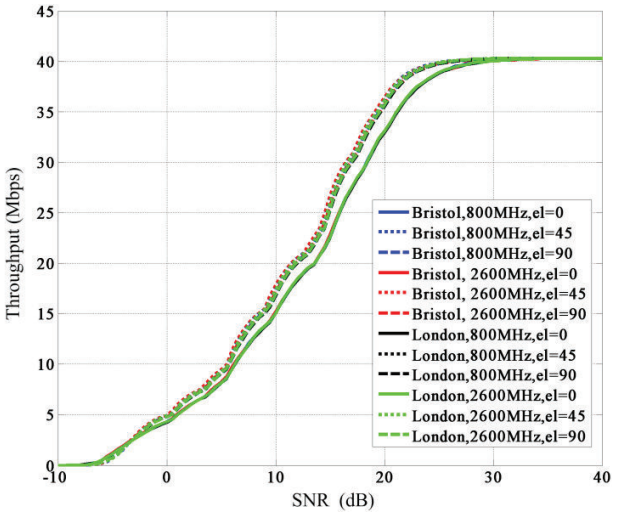

Fig. 5. Throughput envelope of 10 MCS averaged over all UEs and BSs.

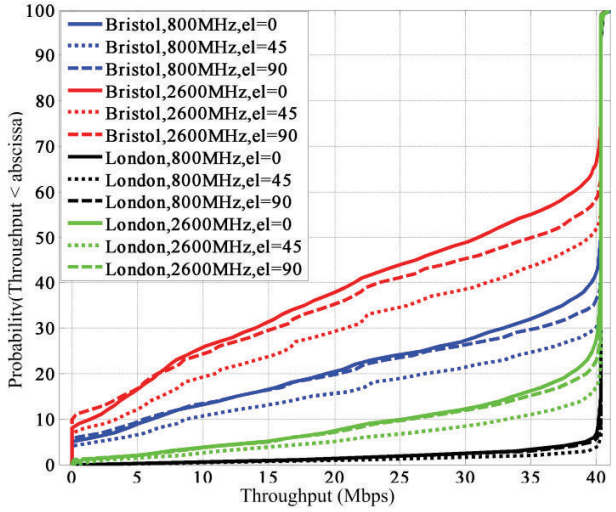

Fig. 6. CDF of UEs throughput for all UEs and BSs.

TABLE IV
TOTAL NUMBER OF UES IN THE STUDY

City	Frequency (MHz)	Number of UE
Bristol	800	13,814
	2600	11,649
London	800	16,346
	2600	16,276

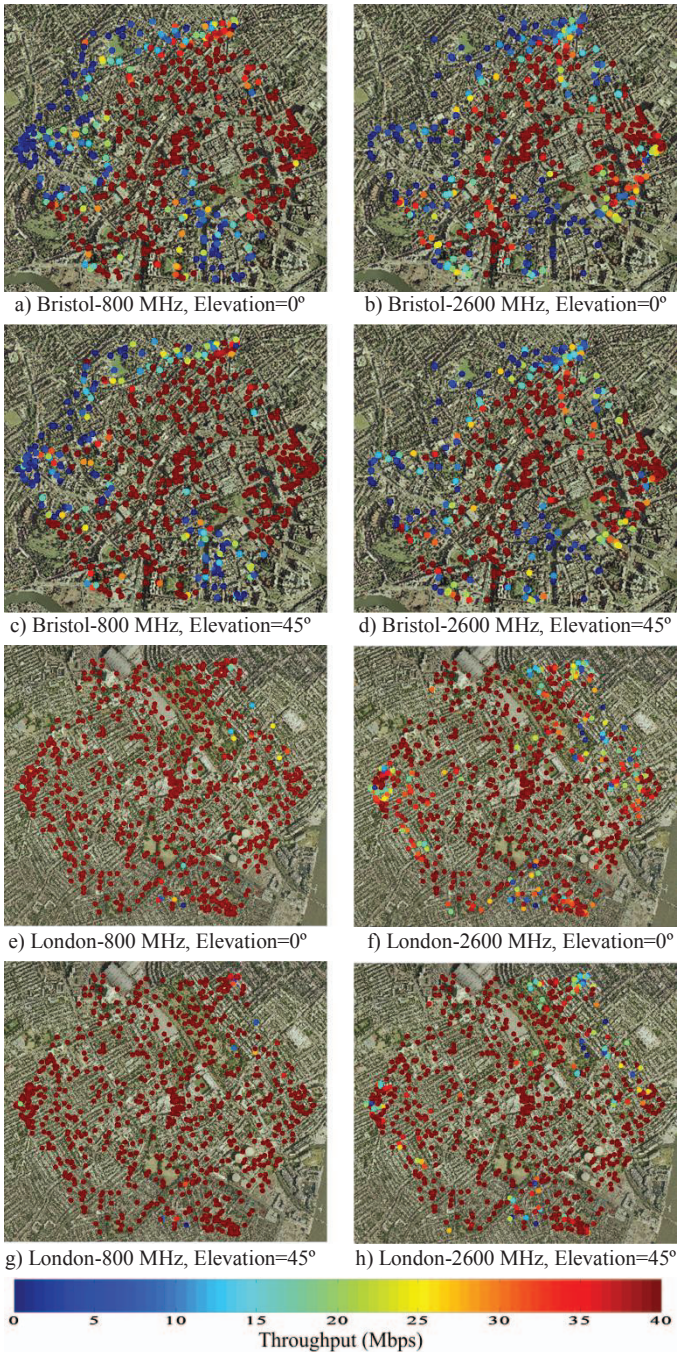

Fig. 7. Throughput coverage map of Bristol and London for different frequencies and UE antenna orientations.

V. CONCLUSIONS

This paper has presented propagation channel statistics for a large number of UEs in two different frequency bands, two different UK cities, and three different UE antenna elevation orientations. An RBIR abstraction model for the LTE-Advanced downlink physical layer was first verified and then used to determine the throughput versus SNR at each UE. The required simulation time at each UE location was reduced by a factor of more than 300 using the RBIR process. Higher throughput was observed in the TVWS band due mainly to reduced path loss. Depending on the frequency band and the nature of the urban area, a UE antenna elevation orientation of 45º was shown to offer higher throughputs compared to elevation rotations of 0º and 90º.

The efficiency of CA to increase macro cell capacity was shown to depend on the urban topography around the base station.

ACKNOWLEDGMENTS

A. Ameen would like to thank the University of Sulaimani and the Ministry of Higher Education and Scientific Research in Kurdistan of Iraq for sponsoring this study.

REFERENCES

[1] E. Dahlman, S. Parkvall, and J. Skold, *4G LTE/LTE-Advanced for Mobile Broadband*. Oxford: Elsevier/Academic Press, 2011.

[2] 3GPP TR 36.850: "Inter-band Carrier Aggregation", V11.0.0, March 2013.

[3] X. Zhu, A. Doufexi, and T. Kocak, "Throughput and Coverage Performance for IEEE 802.11ad Millimetre-Wave WPANs", *73rd IEEE Vehicular Technology Conference,* May 2011.

[4] R. Saeed and S. Shellhammer, *TV White Space Spectrum Technologies: Regulations, Standards, and Applications*, CRC Press, 2012.

[5] OFCOM, "Digital Dividend: Cognitive Access", Statement on License Exempting Cognitive Devices using Interleaved Spectrum, July 2009.

[6] S. Lim, H. Jung, and B. Jeong, "Efficient Multi-Channel Signal Detection Algorithms for Cognitive Radio Systems in TV White Space" *IEEE International Symposium on a World of Wireless, Mobile and Multimedia Networks,* June 2012.

[7] E. Tameh and A. Nix, "The Use of Measurement Data to Analyse the Performance of Rooftop Diffraction and Foliage Loss Algorithms in a 3-D Integrated Urban/Rural Propagation Model", *48th IEEE Vehicular Technology Conference*, May 1998.

[8] 3GPP TR 25.996, "Spatial Channel Model for Multiple Input Multiple Output (MIMO) Simulations", V11.0.0, September 2009.

[9] E. Mellios, A. Nix, and G. Hilton, "Ray-tracing Urban Macro-cell Propagation Statistics and Comparison with WINNER II/+ Measurements and Models" *Loughborough Antennas and Propagation Conference,* November 2012.

[10] E. Mellios, Z. Mansor, G. Hilton, A. Nix, and J. McGeehan, "Impact of Antenna Pattern and Handset Rotation on Macro-cell and Pico-cell Propagation in Heterogeneous LTE networks", *IEEE International Symposium on Antennas and Propagation* , Jul 2012.

[11] D. Hall, "Interference Characterisation and Mitigation in Mobile Broadband Wireless Networks", Ph.D. dissertation, Department of Electrical and Electronic Engineering, University of Bristol, Bristol, UK, 2011.

[12] A. Doufexi, E. Tameh, A. Nix, S. Armour, and A. Molina, "Hotspot Wireless LANs to Enhance the Performance of 3G and Beyond Cellular Networks," *Communications Magazine, IEEE*, vol.41, no.7, pp.58-65, July 2003.

[13] 3GPP TS 36.942, "Evolved Universal Terrestrial Radio Access (E-UTRA): Radio Frequency (RF) System Scenarios", V10.2.0, Dec 2010.